Exploring the Mechanism of Agonist Efficacy: A Relationship between Efficacy and Agonist Dissociation Rate at the Muscarinic M$_3$ Receptor

David A. Sykes, Mark R. Dowling, and Steven J. Charlton

Novartis Institutes for Biomedical Research, Horsham, West Sussex, United Kingdom

Received December 24, 2008; accepted June 4, 2009

ABSTRACT

Although there are several empirical approaches that enable the comparison of relative agonist efficacy, the molecular basis that underlies differences in the ability of G protein-coupled receptor agonists to elicit a response is still largely unexplained. Several models have been described that incorporate the kinetics of receptor-mediated initiation of the G protein cycle, but these have not directly addressed the influence of agonist-binding kinetics. To test this, we investigated the relationship between the efficacy of seven M$_3$ muscarinic receptor agonists and their rate of dissociation (k_{off}) from the M$_3$ receptor. The association and dissociation rate constants of the agonists were determined using a *l*-[*N*-methyl]-[^{3}H]scopolamine methyl chloride competition binding assay in the presence of GTP. The agonists displayed a range of association and dissociation rates. Relative agonist efficacy was measured at two points after M$_3$ receptor activation: the stimulation of guanosine 5'-*O*-(3-[^{35}S]thio)triphosphate binding to Gα subunits, and the subsequent increase in intracellular calcium levels. These experiments revealed a range of intrinsic efficacy, from the low-efficacy pilocarpine and oxotremorine to high-efficacy acetylcholine. There was no relationship between agonist efficacy and the equilibrium binding affinity of each agonist (K_d). When efficacy was compared with the dissociation rate constant, however, the two were highly correlated, suggesting a relationship between the duration of agonist binding at the receptor and the intrinsic efficacy. These data suggest that kinetic models incorporating the mean lifetime of specific complexes will be required to fully explain the nature of agonist efficacy.

Efficacy is defined as the ability of a ligand to elicit a response upon binding to a receptor (Stephenson, 1956) and is arguably the most important parameter for optimization in novel agonist drugs. To date, efficacy has largely been treated as an empirical term, and several approaches comparing equilibrium binding to functional potency have been described for its measurement (Black and Leff, 1983; Ehlert, 1985). Although they provide a pragmatic approach to ranking ligands, these methods make no attempt to explain the molecular mechanism behind efficacy. One of the first attempts to provide a mechanistic explanation for agonist efficacy was by Paton (1961), termed "rate theory." This model considers that excitation by a stimulant drug is proportional to the rate of drug-receptor combination rather than to the proportion of receptors occupied by the drug. In this case, once the receptor has been activated and the signal trans-

duced, it must be reset by dissociation of the agonist before another activation event can be initiated by binding of another agonist molecule. Thus, a high-efficacy ligand would dissociate rapidly from the receptor, allowing another agonist to bind rapidly, whereas a low-efficacy agonist would dissociated more slowly from the receptor, acting effectively as a competitive antagonist against other agonist molecules. This model was proposed after the observation that efficacy and offset for a series of ligands at the guinea pig ileum were negatively correlated.

Since then, however, models have been developed that describe efficacy in terms of the ability to stabilize an active receptor conformation. Perhaps the most widely used is the two-state model, originally described for activation of ion channels (Del Castillo and Katz, 1957) but since adapted for use with G protein-coupled receptors (Karlin, 1967; Colquhoun, 1973; Thron, 1973; Leff, 1995). In this model, the efficacy of an agonist is dependent on its affinity for R* (active conformation) over R (inactive state). Thus, an agonist that preferentially binds R* will drive the equilibrium

ABBREVIATIONS: I.A., intrinsic activity; CHO, Chinese hamster ovary; HBSS, Hanks' balanced salt solution; [^{3}H]NMS, *l*-[*N*-methyl]-[^{3}H]scopolamine methyl chloride; [^{35}S]GTPγS, guanosine 5'-*O*-(3-[^{35}S]thio)triphosphate; BSA, bovine serum albumin; AM, acetoxymethyl ester; UK14,304, 6-quinoxalinamine, 5-bromo-*N*-(4,5-dihydro-1H-imidazol-2-yl)-.

between the two states toward the active conformation and will display high efficacy. If the binding affinity is higher for R than R*, an agonist will exhibit negative efficacy by driving the equilibrium toward the inactive state. A full spectrum of efficacy can be established between these two extremes, governed by the differential in affinity for the two receptor states. This model predicts that affinity and efficacy are inextricably linked (Colquhoun, 1998), although unlike Paton's rate theory, higher relative affinity at the active conformation would result in a higher efficacy agonist. This model has been extended to include the presence of G proteins in the extended ternary complex model (Samama et al., 1993) or the more thermodynamically complete cubic ternary complex model (Weiss et al., 1996). The assumption of equilibrium in these models is, however, a simplification, because the ternary complex is not stable and does not accumulate in the presence of agonist.

To address this, Waelbroeck et al. (1997) proposed a kinetic model in which the receptor acts as an enzyme that catalyzes GDP/GTP exchange on the G protein and the agonist as an allosteric activator. In this model, once the GTP-bound G protein dissociates, the agonist-bound receptor is free to catalyze another reaction cycle. A similar kinetic approach has since been described for the cubic ternary complex model, in which the model was modified to include the breakdown of the ternary complex and recycling of G protein (Shea et al., 2000; Kinzer-Ursem and Linderman, 2007). Like the kinetic model of Waelbroeck et al. (1997), providing the agonist remains bound to receptor, it is able to catalyze multiple rounds of the G protein cycle.

According to these newer kinetic models, it may be hypothesized that the mean receptor residency time of a rapidly dissociating agonist may not be long enough to facilitate a full, productive turn of the cycle (thus showing low efficacy), whereas a slowly dissociating agonist may catalyze several cycles before dissociating, thereby displaying higher efficacy (Scheme 1). To test this, we determined the dissociation rates of seven muscarinic M_3 receptor agonists and compared them with two empirical measures of agonist efficacy, intrinsic activity (I.A.) and τ, from the operational model of Black and Leff (1983), in an effort to test whether the observed residency of an agonist at the receptor is directly linked to apparent efficacy.

Materials and Methods

Chemicals and Reagents. l-[N-methyl]-[³H]Scopolamine methyl chloride ([³H]NMS; specific activity, 80–90 Ci/mmol) and guanosine
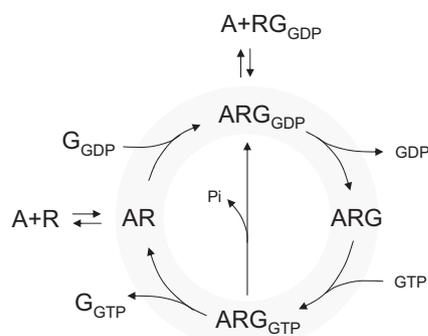
Scheme 1. Graphical representation of agonist-mediated G protein activation.

5′-O-(3-[³⁵S]thio)triphosphate ([³⁵S]GTPγS; specific activity, >1000 Ci/mmol) and wheat germ agglutinin SPA beads were obtained from Amersham Biosciences (GE Healthcare, Chalfont St. Giles, Buckinghamshire, UK). The 96-deep-well plates and 500-cm² cell culture plates were purchased from Thermo Fisher Scientific (Waltham, MA). The 96-well GF/B filter plates were purchased from Millipore (Watford, UK). HBSS, sodium bicarbonate, EDTA, sodium chloride, HEPES, dimethyl sulfoxide, BSA, GTP, GDP, saponin, probenecid, acetylcholine chloride, carbachol chloride, methacholine chloride, bethanechol chloride, oxotremorine-M, oxotremorine sesquifumarate, and pilocarpine hydrochloride were obtained from Sigma Chemical Co Ltd. (Poole, UK). Brilliant black was obtained from ICN Biomedicals Inc. (Solon, OH). Pluronic acid, Fluo-4-AM and all cell culture reagents were purchased from Invitrogen (Paisley, UK).

Cell Culture. Chinese hamster ovary (CHO) cells transfected with the cDNA encoding the human M_3 (CHO-M_3) muscarinic acetylcholine receptor was a kind gift from Professor S. R. Nahorski (Department of Cell Physiology and Pharmacology, University of Leicester, Leicester, UK). CHO cells were grown in minimum essential medium supplemented with 10% newborn calf serum. Cells were maintained at 37°C in 5% CO_2/humidified air. Cells were routinely split 1:10, using trypsin-EDTA to lift cells, and were not used in assays beyond passage 40.

Cell Membrane Preparation. CHO cells expressing the M_3 muscarinic acetylcholine receptor were grown to 80 to 90% confluence in 500-cm² cell culture plates at 37°C in 5% CO_2. All subsequent steps were conducted at 4°C to avoid receptor degradation. The cell culture media were removed, and ice-cold buffer [1 × 10 ml: 10 mM HEPES, 0.9% (w/v) NaCl, and 0.2% (w/v) EDTA, pH 7.4] was added to the cells, which were then scraped from the plates into a 50-ml Corning tube (Corning Inc., Corning, NY) and subsequently centrifuged at 250*g* for 5 min to allow a pellet to form. The supernatant fraction was aspirated, and 10 ml per 500-cm² tray of wash buffer (10 mM HEPES and 10 mM EDTA, pH 7.4) was added to the pellet. This was homogenized using an electrical homogenizer Ultra-Turrax (Ika-Werk GmbH & Co. KG, Staufen, Germany) (position 6, 4 × 5-s bursts) and subsequently centrifuged at 48,000*g* at 4°C (Beckman Avanti J-251 Ultracentrifuge; Beckman Coulter, Fullerton, CA) for 30 min. The supernatant was discarded, and the pellet was rehomogenized and centrifuged as described above in wash buffer. The final pellet was suspended in ice-cold 10 mM HEPES and 0.1 mM EDTA, pH 7.4, at a concentration of 5 to 10 mg/ml. Protein concentration was determined by the Bio-Rad Protein Assay (Bio-Rad Laboratories, Hercules, CA) based on the method of Bradford (1976) using BSA as a standard, and aliquots were maintained at −80°C until required.

Common Procedures Applicable to All Radioligand Binding Experiments. All radioligand experiments were conducted in 96-deep-well plates in assay binding buffer HBSS, pH 7.4, with GTP (100 μM) at 37°C. In all cases, nonspecific binding was determined in the presence of 1 μM atropine. After the indicated incubation period, bound and free [³H]NMS were separated by rapid vacuum filtration using a FilterMate Cell Harvester (PerkinElmer Life and Analytical Sciences, Beaconsfield, UK) onto 96-well GF/B filter plates and rapidly washed three times with ice-cold 20 mM HEPES, pH 7.4. After drying (>4 h), 40 μl of Microscint 20 (PerkinElmer Life and Analytical Sciences) was added to each well, and radioactivity was quantified using single-photon counting on a TopCount microplate scintillation counter (PerkinElmer Life and Analytical Sciences). Aliquots of [³H]NMS were also quantified accurately to determine how much radioactivity was added to each well using liquid scintillation spectrometry on an LS6500 scintillation counter (Beckman Coulter). In all experiments, total binding never exceeded more than 10% of that added, limiting complications associated with depletion of the free radioligand concentration (Carter et al., 2007).

[³H]NMS Saturation Binding. Binding was performed with a range of concentrations of [³H]NMS (~0.004–8 nM) to construct saturation binding curves, as described by Dowling and Charlton

(2006). CHO-M$_3$ cell membranes (10 μg/well) were incubated in 96-deep-well plates at 37°C in assay binding buffer with gentle agitation for 3 h to ensure that equilibrium was reached. Because of the low concentrations of [³H]NMS used, the assay volume was increased to 1.5 ml to avoid significant ligand depletion.

Determination of Agonist K_i. To obtain affinity estimates of unlabeled agonists, [³H]NMS competition experiments were performed at equilibrium. [³H]NMS was used at a concentration of approximately 350 pM (~40,000 c.p.m. in a volume of 1.5 ml) such that the total binding never exceeded more than 10% of that added. [³H]NMS was incubated in the presence of the indicated concentration of unlabeled agonist and CHO cell membranes (10 μg/well) at 37°C with agitation for 3 h.

Determination of the Association Rate (k_{on}) and Dissociation Rate (k_{off}) of [³H]NMS. To determine the k_{on}, the k_{ob} was calculated at three different concentrations of [³H]NMS (approximately 222, 666, and 2000 pM; exact concentrations were calculated in each experiment using liquid scintillation counting) The experiment was initiated ($t = 0$) by the addition of CHO-M$_3$ cell membranes (10 μg/well) to [³H]NMS in assay binding buffer (final assay volume, 500 μl) and incubated with gentle agitation. Free [³H]NMS was separated at multiple time points to construct association kinetic curves. Care was taken to ensure that saturation for each experiment was reached before the experiment was terminated. After incubation, bound radioactivity was separated from free by rapid filtration, plates were left to dry, and radioactivity was quantified (as described previously). The kinetic rate constants for [³H]NMS were calculated as described below under Data Analysis.

Competition Kinetics. The kinetic parameters of unlabeled agonists were assessed using a competition kinetic binding assay as described by Dowling and Charlton (2006). Approximately 2 nM [³H]NMS (a concentration that avoids ligand depletion in this assay volume) was added simultaneously with the unlabeled compound to CHO-M$_3$ membranes (10 μg/well) in 500 μl of assay buffer. The degree of [³H]NMS bound to the receptor was assessed at multiple time points by filtration harvesting and liquid scintillation counting, as described previously. Nonspecific binding was determined as the amount of radioligand bound to the filters and membrane in the presence of atropine (1 μM) and was subtracted from each time point, meaning that $t = 0$ was always equal to 0. Each time point was conducted on the same 96-deep-well plate incubated at 37°C with constant agitation. Reactions were considered stopped once the membranes reached the filter, and the first wash was applied within 1 s. Three different concentrations of unlabeled competitor were tested to ensure the rate parameters calculated were independent of ligand concentration. All compounds were tested at 10-, 3-, and 1-fold of their respective K_i, and data were globally fitted using eq. 2 to simultaneously calculate k_{on} and k_{off}.

Measurement of Changes in Cytoplasmic [Ca²⁺] Using a Fluorometric Imaging Plate Reader. CHO-M$_3$ cells were seeded into 96-well black plates (Costar; Corning Life Sciences, Acton, MA) at 50,000 cells/well in 100 μl of tissue culture medium, supplemented as above, and incubated at 37°C/5% CO$_2$ for approximately 24 h. On the day of the experiment, the cells were loaded in HBSS without phenol red containing 0.1% (w/v) BSA, HEPES (20 mM), Fluo-4-AM [2 μM, 50 μg of Fluo-4-AM dissolved in 44 μl of dimethyl sulfoxide/ Pluronic acid (1:1)], probenecid (250 μM), and brilliant black (100 μM), and incubated at 37°C/5% CO$_2$ for 30 min. Agonist-induced changes in Ca²⁺ concentration were monitored using fluorometric imaging plate reader (Molecular Devices, Sunnyvale, CA). The laser intensity on the fluorometric imaging plate reader was set between 0.4 and 0.5 W, a level sufficient to obtain basal fluorescence of ~10,000 U. Basal fluorescence was monitored for 10 s before the addition of 50 μl of muscarinic agonist at a speed of 50 μl/s, and the fluorescence change was monitored for 5 min. Responses to agonist were expressed as the change in fluorescence from baseline to peak. The maximum fluorescence was taken as the highest point of the

initial peak after agonist addition. The minimum fluorescence was taken as the background fluorescence before agonist addition.

[³⁵S]GTPγS Binding Assay. The [³⁵S]GTPγS binding assays were performed in white 96-well optiplates in a final volume of 250 μl as follows. In brief, the frozen cell membranes were thawed and resuspended in GTPγS binding buffer [HBSS containing 20 mM HEPES, 10 μg/ml saponin, and 0.1% (w/v) BSA, pH 7.4]. Membranes (30 μg/well), GDP (1 μM), SPA beads (1 mg/well), [³⁵S]GTPγS (300 pM), and the muscarinic M$_3$ agonists at a range of concentrations were added to the plates. Plates were incubated for a further 1 h at 30°C with shaking before centrifugation at 3000 rpm (Jouan B4i; Jouan, St. Herblain, France) for 3 min and then read on the Top-Count (30 s/well).

Data Analysis. Because the amount of radioactivity varied slightly for each experiment (<5%), data are shown graphically as the mean $\pm$ range for individual representative experiments, whereas all values reported in the text and tables are mean $\pm$ S.E.M. for the indicated number of experiments. All experiments were analyzed by either linear or nonregression using Prism 4.0 (GraphPad Software Inc., San Diego, CA). Competition displacement binding data were fitted to sigmoidal (variable slope) curves using a four-parameter logistic equation:

$$Y = \text{Bottom} + (\text{Top} - \text{Bottom})/(1 + 10^{(\log EC_{50} - X) \, \text{Hill coefficient}}) \quad (1)$$

IC$_{50}$ values obtained from the inhibition curves were converted to K_i values using the method of Cheng and Prusoff (1973).

[³H]NMS association data were globally fitted to the following equation to determine a single best-fit estimate for k_{on} and k_{off}:

$$K_{ob} = [\text{radioligand}] \cdot k_{on} + k_{off} \quad (2)$$

Association and dissociation rates for unlabeled agonists were calculated by simultaneously fitting the data for each competitor concentration to eq. 3:

$$K_A = k_1[L] + k_2$$

$$K_B = k_3[I] + k_4$$

$$S = \sqrt{(K_A - K_B)2 + 4 \cdot k_1 \cdot k_3 \cdot [L] \cdot [I] \cdot le^{-18})}$$

$$K_F = 0.5 \cdot (K_A + K_B + S)$$

$$K_S = 0.5 \cdot (K_A + K_B - S)$$

$$\text{DIFF} = K_P - K_S$$

$$Q = \frac{B_{max} \cdot K_1 \cdot [L] \cdot le^{-9}}{\text{DIFF}}$$

$$Y = Q \cdot \left(\frac{K_4 \cdot \text{DIFF}}{K_F \cdot KS} + \frac{k_4 - K_F}{K_F} e^{(-K_1 \cdot X)} - \frac{K_4 - K_S}{K_S} e^{(-K_S \cdot X)} \right) \quad (3)$$

where X is time (minutes), Y is specific binding (counts per minute), K_1 is k_{on} [³H]NMS, K_2 is k_{off} [³H]NMS, [L] is the concentration of [³H]NMS used (nanomolar), and [I] is the concentration of unlabeled agonist (nanomolar). Fixing the above parameters allowed the following to be simultaneously calculated: B_{max} is total binding (counts per minute), k_3 is the association rate of unlabeled ligand (M^{-1} · min^{-1}) or k_{on}, and k_4 is the dissociation rate of unlabeled ligand (min^{-1}) or k_{off}.

To evaluate the relative efficacy of agonists that produced the same maximal response in the calcium assay, data were fitted to the operational model of Black and Leff (1983). This model describes the correlation between a biological effect E and agonist concentration [A] as a function of three parameters: E_m, K_A, and τ:

$$E = \frac{E_m \cdot \tau \cdot [A]}{K_A + [A] + \tau \cdot [A]} \quad (4)$$

where E_m, or the operational maximum, represents the maximum possible effect in the tissue, K_A is the dissociation constant of the agonist and τ is the operational efficacy or the transducer ratio. When eq. 4 was applied to data, [A] was varied according to experimental design, K_A was fixed to the value obtained in competition binding assays (run in conditions identical with the functional experiments), and E_m was globally fitted across all data sets, leaving τ as the only term fitted individually for each agonist.

Results

Characterization of M_3 Receptor-Expressing CHO Cell Line. Specific [³H]NMS binding to muscarinic receptors in CHO-M_3 membranes was saturable and best described by the interaction of the radioligand with a single population of high-affinity binding sites. The expression level of the M_3 CHO-cell line was estimated from the B_{max} in [³H]NMS saturation binding as 3.0 ± 0.4 pmol/mg ($n = 4$). From these studies, the equilibrium dissociation constant (K_d) of [³H]NMS was determined to be 289 ± 13 pM ($n = 4$).

[³H]NMS Competition Binding Studies. The CHO-M_3 receptor binding profile of the seven muscarinic agonists was determined in buffer containing GTP (100 μM). GTP was included to ensure that agonist binding only occurred to the uncoupled form of the M_3 receptor. All seven agonists produced concentration-dependent inhibition of specific [³H]NMS binding. Examples of competition curve data are shown in Fig. 1, and pK_i values were determined as shown in Table 1. Slope parameter estimates for all agonists tested
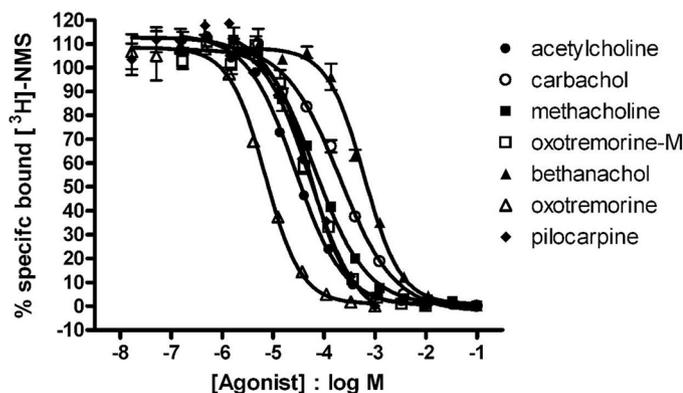
Fig. 1. Competition between [³H]NMS and increasing concentrations of muscarinic agonists for muscarinic M_3 receptors in CHO cell membranes. Experiments were conducted in HBSS at 37°C. Because the total binding varied, data are shown as mean ± range from a representative of four or more experiments performed in duplicate and plotted as the percentage of specific bound.

were not different from unity, suggesting that binding occurs to a single population of receptor.

Characterization of [³H]NMS Kinetic Parameters. A family of association kinetic curves was constructed using a range of [³H]NMS concentrations. Each association curve was monitored until equilibrium was achieved (Fig. 2). The data were globally fitted to eq. 2 to derive a single best-fit estimate for the k_{on} and k_{off} of [³H]NMS. Mean values obtained for the on- and off-rates were $9.26 \pm 0.69 \times 10^8$ M^{-1} · min^{-1} and 0.30 ± 0.05 min^{-1}, respectively. The kinetically derived K_d (k_{off}/k_{on}) calculated from the mean values for the individual experiments (341 ± 72 pM) was in good agreement with the value obtained from [³H]NMS saturation experiments of 289 ± 13 pM.

Competition Kinetic Binding. This method models the binding between two ligands, one labeled and one unlabeled, competing for the same receptor site. Representative curves for acetylcholine and pilocarpine are shown in Fig. 3, A and B, respectively. The pattern of [³H]NMS binding over time was dependent on the off-rate of the competing agonist. [³H]NMS association in the presence of more slowly equilibrating competitors (slow off-rate) was two-phase. The initial, rapid phase was equivalent to the rate of association of radioligand alone and represents binding to free receptors. The second phase represents equilibration of the two ligands with the receptor and was significantly slower. In the presence of more rapidly equilibrating agonists, the first phase of [³H]NMS binding was much less apparent because the majority of free receptors (at $t = 0$) were occupied first by the competitor. Progression curves for [³H]NMS alone and in the presence of three different concentrations of competitor were globally fitted to eq. 3, enabling the calculation of both k_{on} (k_3) and k_{off} (k_4) for each of the agonists, as reported in Table 1. Because the k_{off} values were similar across the cohort, we tested whether the data were sufficient to discriminate between the agonists. The quality of fit was worse when the k_{off} was fixed to any value outside that was predicted by simultaneous fitting. There was a much larger difference in k_{on} values between the agonists. Interestingly, these correlated well with the K_d ($r^2 = 0.92$, $p < 0.001$ for $\log k_{on}$ versus pK_d), suggesting that it is the on-rate that governs the equilibrium affinity of these agonists. To validate the rate constants, the kinetically derived K_d values (k_{off}/k_{on}) were compared with the affinity constant (K_i) obtained from equilibrium competition binding experiments (Fig. 4). Although there was a very good correlation ($r^2 = 0.99$) between these two values,

TABLE 1

Binding parameters for agonists at the human M_3 muscarinic receptor derived from equilibrium and kinetic competition experiments with [³H]NMS

Data are mean ± S.E.M. from four to six separate experiments.

Agonist	Kinetic				Equilibrium	
	k_{on}	k_{off}	$t_{1/2}$	pK_d (k_{off}/k_{on})	pK_i	Slope
	$M^{-1} \cdot min^{-1}$	min^{-1}	s			
Acetylcholine	$1.82 \pm 0.32 \times 10^5$	5.6 ± 0.6	7.8 ± 0.9	4.50 ± 0.05	4.87 ± 0.04	-1.04 ± 0.02
Carbachol	$0.58 \pm 0.01 \times 10^5$	8.8 ± 1.1	6.3 ± 1.7	3.77 ± 0.06	4.09 ± 0.03	-0.98 ± 0.02
Methacholine	$1.20 \pm 0.07 \times 10^5$	7.9 ± 0.8	6.0 ± 1.0	4.21 ± 0.04	4.52 ± 0.05	-1.03 ± 0.07
Oxotremorine M	$1.43 \pm 0.25 \times 10^5$	6.9 ± 1.1	7.2 ± 1.5	4.33 ± 0.03	4.61 ± 0.04	-1.03 ± 0.05
Bethanachol	$0.48 \pm 0.07 \times 10^5$	13.3 ± 2.2	3.7 ± 1.0	3.57 ± 0.04	3.71 ± 0.04	-1.03 ± 0.05
Oxotremorine	$5.12 \pm 1.56 \times 10^6$	17.6 ± 2.6	2.6 ± 0.5	5.36 ± 0.11	5.61 ± 0.01	-1.04 ± 0.03
Pilocarpine	$4.47 \pm 0.53 \times 10^5$	15.3 ± 2.3	3.0 ± 0.4	4.50 ± 0.06	4.78 ± 0.06	-0.99 ± 0.03

there was a small (approximately 2-fold) but consistent difference for all of the agonists.

Measurement of [^{35}S]GTPγS Binding Activity. Each ligand stimulated the incorporation of [^{35}S]GTPγS into the CHO-M$_3$ membranes, displaying a range of potency and intrinsic activity (Fig. 5A and Table 2). When the data were
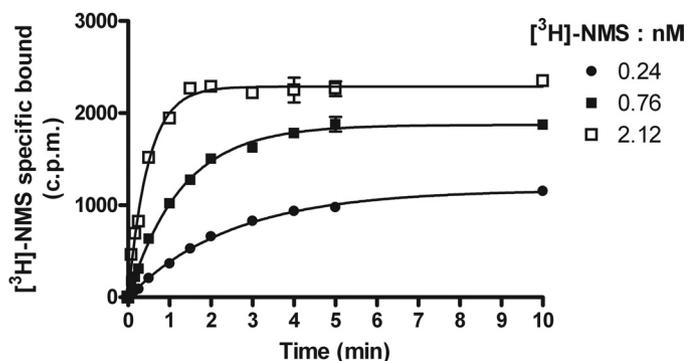
Fig. 2. Characterization of the kinetic parameters of [^{3}H]NMS. The k_{on} and k_{off} were determined by incubation of CHO-M$_3$ cell membranes (10 μg/well) with indicated concentrations of [^{3}H]NMS for various time points. Experiments were conducted in HBSS at 37°C. Data were globally fitted to the association kinetic model to derive a single best-fit estimate for the k_{on} and k_{off}. Data are shown as mean ± range from a representative of four or more experiments performed in duplicate and plotted as specific bound.
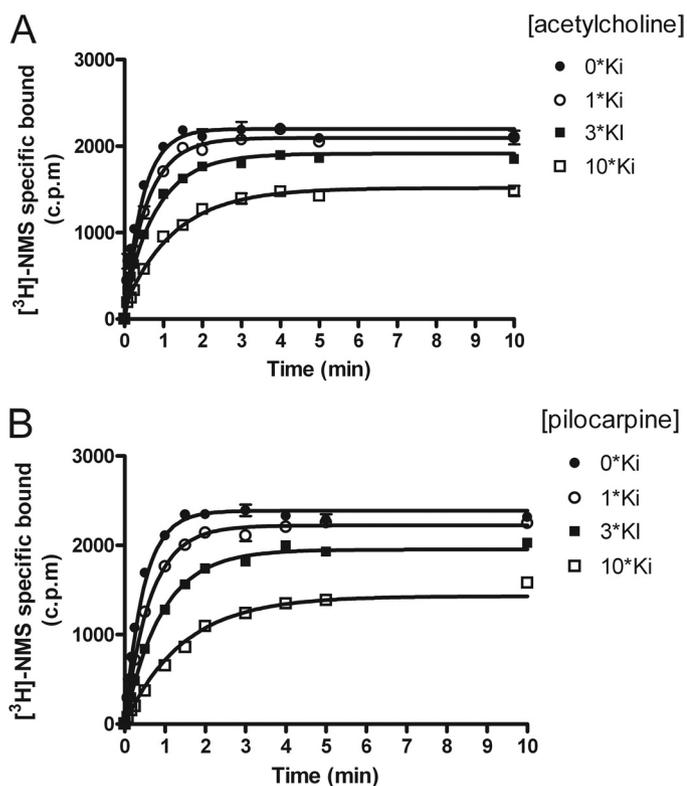
Fig. 3. Example [^{3}H]NMS competition kinetic curves in the presence of acetylcholine (A) or pilocarpine (B). CHO-M$_3$ membranes were incubated with ~2 nM [^{3}H]NMS and either 0, 1, 3, and 10-fold K_i of competitor. Plates were incubated at 37°C with constant shaking for the indicated time points, and nonspecific binding levels were determined in the presence of atropine (1 μM). Data were globally fitted to the equations described under *Materials and Methods* to calculate k_{on} and k_{off} values for the unlabeled agonists. The whole data set is summarized in Table 1. Because the total binding varied from experiment to experiment, data are presented as the mean ± range from a representative of four or more experiments performed in duplicate and plotted as specific bound.

simultaneously fitted to the operational model, τ values were very low, suggesting that there was little if any receptor reserve at this early step in the transduction pathway.

Measurement of Changes in Cytoplasmic [Ca^{2+}]. All seven of the muscarinic agonists tested stimulated an increased intracellular calcium concentration in CHO-M$_3$ cells (Fig. 5B). The maximal responses to these ligands did not differ significantly from each other ($p < 0.05$) despite the fact that some of these ligands were partial agonists in the GTPγS assay. This is probably because of the greater degree of amplification associated with calcium signaling. Because relative efficacy could not be determined in this system by comparing maximal agonist responses, the data were fitted to an operational model that compares binding affinity to functional potency to calculate τ, a value that can be used to compare relative efficacies of agonists when tested in the same system (Black and Leff, 1983). A range of τ values were obtained that broadly agreed with the rank order of intrinsic activity from the [^{35}S]GTPγS binding assay (Table 2).

Relationship between Agonist Efficacy and k_{off}. There was no relationship between the affinity (K_d) of the seven agonists tested here and their relative efficacy determined either in the calcium assay ($r^2 = 0.05$, $p = 0.63$) or [^{35}S]-GTPγS ($r^2 = 0.07$, $p = 0.57$) (Fig. 6, A and C, respectively). Likewise, there was no relationship between k_{on} and efficacy ($r^2 = 0.23$, $p = 0.28$, and $r^2 = 0.32$, $p = 0.19$ from Ca^{2+} and GTPγS data, respectively) (correlation not shown). However, when the efficacy of each agonist was compared with its dissociation rate constant (k_{off}), a highly significant correlation was obtained, with the highest efficacy ligands having the slowest dissociation rates. This correlation was observed when k_{off} was compared with either τ from the calcium assay ($r^2 = 0.98$, $p < 0.0001$) or I.A. from the GTPγS data ($r^2 = 0.95$, $p = 0.0002$), suggesting that the dissociation rate for these muscarinic agonists plays an important role in defining efficacy at the M$_3$ receptor (Fig. 6, B and D).

Discussion

The aim of this study was to investigate whether the observed rate of agonist dissociation is related to observed efficacy, such that the receptor residency time of a rapidly dissociating agonist is not always long enough to facilitate a
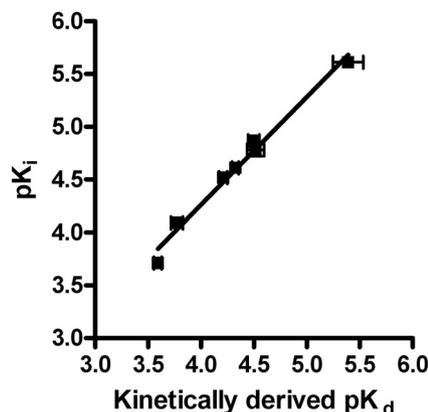

Fig. 4. Correlation between pK_i and kinetically derived pK_d for the seven test agonists. pK_i values were taken from [^{3}H]NMS competition binding experiments at equilibrium (see Fig. 1). The values comprising the kinetically derived K_d (k_{off}/k_{on}) were taken from the experiments in Fig. 3. Data shown as mean S.E.M. ($n = \geq 4$).

full, productive G protein activation event (thus showing low efficacy), whereas a slowly dissociating agonist may catalyze several G protein activation cycles before dissociating, thereby displaying higher efficacy.

To assess relative agonist efficacy, we measured M_3-mediated activation at two different points: direct activation of $G\alpha$ subunits using GTPγS binding, and the subsequent release of intracellular calcium. The agonists displayed different maximal responses in the GTPγS assay but were all maximally effective in the calcium experiments. To determine relative efficacy from the calcium data, we fitted the data to the operational model of Black and Leff (1983). The values obtained using this method were in broad agreement with intrinsic activity measurements from the GTPγS assay.

To determine the dissociation kinetics of the seven agonists, we used a competition kinetic method using a radiolabeled antagonist, [3H]NMS (Dowling and Charlton, 2006). The agonists displayed a range of dissociation rate constants, from 5.6 min^{-1} for acetylcholine to 17.6 min^{-1} for oxotremorine. The off-rate of acetylcholine is moderately faster than that previously described by Kellar et al. (1985) using [3H]acetylcholine (1.04 min^{-1}), but this was performed at 25°C in cerebral cortex and probably represents a mixture of rates from a variety of muscarinic receptor subtypes. The association rate constants of these agonists were significantly slower than those previously reported for antagonists at the M_3 receptor (Dowling and Charlton, 2006). This is contrary to the generally assumed situation that equilibrium affinity is governed predominantly by off-rate and that on-rate is effectively diffusion-limited. It is, however, consistent with previous attempts to measure agonist kinetics at mus-
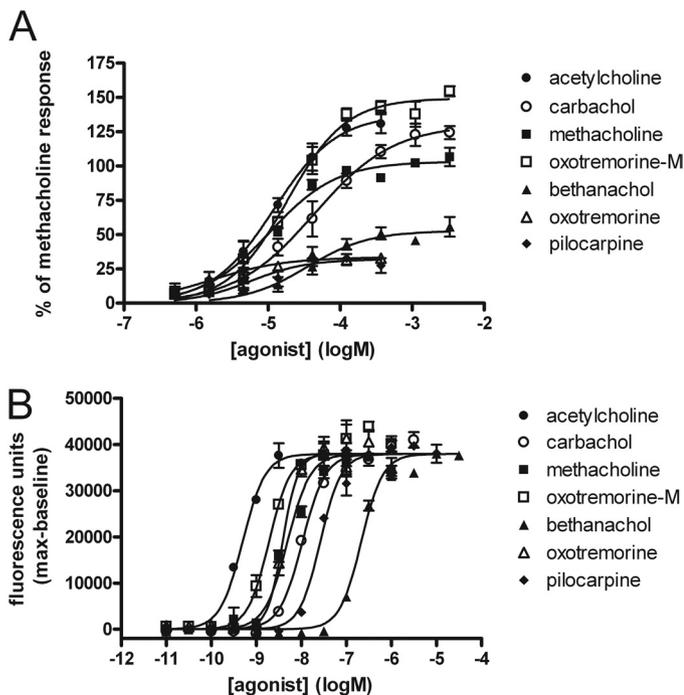
Fig. 5. Concentration-response curves of M_3 muscarinic agonists, measuring GTPγS binding to CHO-M_3 membranes (A) and agonist-induced Ca^{2+} mobilization from CHO-M_3 cells, fitted to the operational model to derive τ (B). For GTPγS binding data are mean ± S.E.M. from four or more separate experiments. For Ca^{2+} mobilization, because measured florescence varied from experiment to experiment, data are presented as mean ± range from a representative of six or more experiments, each performed in duplicate.

TABLE 2
Relative agonist efficacy derived from both [35S]GTPγS binding and calcium release experiments
Data are mean ± S.E.M. from four to six separate experiments.

| Agonist	Calcium Release			GTPγS Binding		
	Potency (pEC$_{50}$)	I.A. (Relative to MCh Response)	Log τ	Potency (pEC$_{50}$)	I.A.(Relative to MCh Response)	Log τ
Acetylcholine	9.33 ± 0.08	1.02 ± 0.04	4.45 ± 0.06	4.99 ± 0.11	1.36 ± 0.05	0.06 ± 0.17
Carbachol	7.98 ± 0.13	1.09 ± 0.05	3.95 ± 0.12	4.64 ± 0.16	1.16 ± 0.05	0.01 ± 0.16
Methacholine	8.52 ± 0.05	1.00	3.97 ± 0.05	5.01 ± 0.03	1.00	−0.11 ± 0.15
Oxotremorine M	8.76 ± 0.09	0.99 ± 0.04	4.14 ± 0.09	5.59 ± 0.10	1.44 ± 0.02	0.19 ± 0.19
Bethanachol	6.77 ± 0.09	0.96 ± 0.05	3.03 ± 0.09	4.62 ± 0.15	0.51 ± 0.04	−0.50 ± 0.10
Oxotremorine	8.47 ± 0.10	1.00 ± 0.03	2.89 ± 0.10	5.59 ± 0.23	0.35 ± 0.02	−0.82 ± 0.15
Pilocarpine	7.72 ± 0.08	0.94 ± 0.03	2.88 ± 0.09	5.05 ± 0.14	0.35 ± 0.04	−0.79 ± 0.12

carinic receptors using competition binding (Schreiber et al., 1985). Although the rate constants described by Schreiber and colleagues can not be directly compared with those obtained in the current study as binding was performed in brain tissue in which multiple muscarinic receptor subtypes exist, the authors demonstrated that at the low-affinity receptor site, the association kinetics were 2 to 5 orders of magnitude lower for agonists compared with antagonists. Sklar and colleagues (1985) made similar observations, in which formyl peptide agonist affinity was largely governed by changes in on-rate rather than off-rate. These reports are consistent with our current observation that it is predominantly the k_{on} that defines the equilibrium affinity of muscarinic agonists.

We have measured the kinetic rate constants in the presence of GTP to remove any pre-existing high-affinity guanine nucleotide-free complexes that may have complicated the analysis (Cohen et al., 1996). It is important to note, however, that we can not definitively ascribe our measured rate constants to a single receptor-G protein complex. Indeed, the two-state model would predict that they comprise a mixture of microscopic rate constants, and that these are directly influenced by the efficacy of the agonist (Colquhoun, 1998). For example, a high-efficacy ligand may more effectively stabilize the activated, high-affinity AR*G$_{(GTP)}$ complex, thereby displaying a slower dissociation rate than an agonist that is unable to promote isomerization to the high-affinity state. Despite this, the observed, macroscopic dissociation rate constants are still useful descriptors of the mean residency time at the receptor, even though they probably represent a mixture of microscopic rate constants.

The data presented in this report are not consistent with the notion that macroscopic equilibrium affinity is correlated to observed efficacy. Rather, we have demonstrated a clear relationship between the efficacy of these muscarinic agonists with the rate of dissociation from the M$_3$ receptor. Can this be reconciled with what we understand about the transduction of receptor signals and the G protein activation cycle? We have shown that the half-life of the agonists tested ranges from 7.8 s for acetylcholine to 2.6 s with oxotremorine. If the efficacy of oxotremorine is limited by its duration at the receptor, the activation interval would need to be in the range of 2.6 s or less so that oxotremorine is not always able to promote a productive turn of the G protein cycle. Whereas the conformational change in receptor and resultant receptor-G protein interaction proceeds very rapidly after agonist binding, in the range of 30 to 50 ms (Lohse et al., 2008), the next step in the activation cycle, GDP release from the α subunit, is slow and represents the rate-limiting step in the G protein cycle. Biddlecome and colleagues (1996) measured the rate of GDP dissociation from Gα$_q$ after carbachol-induced activation by the M$_1$ muscarinic receptor and found that at a saturating concentration of carbachol, GDP dissociation from Gα$_q$ was biphasic with constants of 20 and 1.4 min^{-1}. Because of differences in experimental protocol, it is not possible to directly compare these time constants with those described in the current study, but it suggests that the rate-limiting step in the cycle may occur at a rate similar to the mean residency time of oxotremorine at the M$_3$ receptor (2.6 s). It is therefore possible that not all receptor binding events will last long enough to promote the dissociation of GDP and will not therefore activate a productive turn of the G protein cycle.

Several other groups have made similar observations, albeit comparing just two ligands. Sklar et al. (1985) found that at the formyl peptide receptor, the full agonist FNLPNTL-FL dissociated with a rate constant of 0.35 min^{-1}, whereas the dissociation rate of the partial agonist FMP was much faster
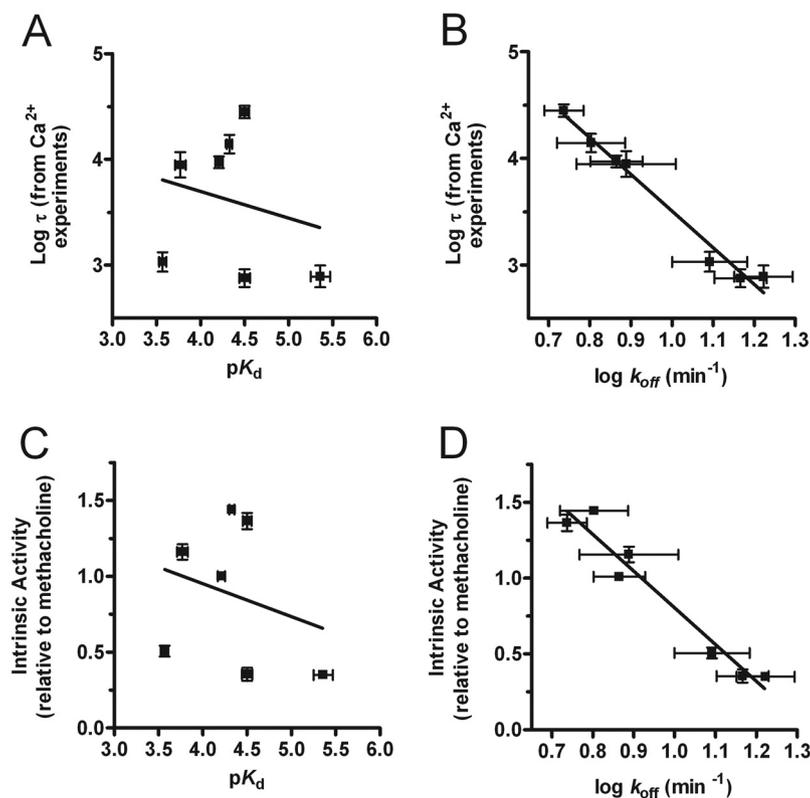
Fig. 6. Correlation of relative agonist efficacy with pK_d and log k_{off}. Logτ, calculated by fitting the operational model to calcium mobilization data (in Fig. 5B), was plotted against pK_d (A) and logk_{off} (B). Intrinsic activity, measured from GTPγS binding as the top of the concentration-response curves (in Fig. 5A), was plotted against pK_d (C) and logk_{off} (D). All data used in these plots are detailed in Tables 1 and 2. Data are expressed as mean ± S.E.M. from four or more separate experiments.

at 5.1 min^{-1}. A similar relationship was reported for the α_2-adrenoceptor agonists UK14,304 and clonidine (Paris et al., 1989). Dissociation experiments using the radiolabeled forms of the agonist showed two rate constants, but in each case, the off-rates of the full agonist UK14,304 were at least 10-fold slower than that of the partial agonist clonidine (0.08 and 1.0 min^{-1} for the fastest phase, respectively). These experiments were performed at 25°C, but more recently, Hoeren and colleagues (2008) have repeated these findings at 37°C, where it was found that the median binding of duration of UK14,304 was approximately 3-fold longer than that of clonidine (79.8 s and 27.6 s, respectively). A key issue with these examples is that in each case, only two ligands were examined. In this present study, we chose a larger cohort of agonists to represent a broader range of intrinsic efficacy. Interestingly, however, rather than an even distribution of efficacy and dissociation rates, the seven ligands examined here tended to form two separate groups of high-efficacy ligands with slow off-rates and lower efficacy ligands with more rapid dissociation kinetics. This could be a chance occurrence that reflects the need to test much larger agonist collections. Alternatively, it could be the nature of the conformational change induced by the agonists, whereby a longer residency provides sufficient time for the receptor to isomerize into the high-affinity state, effectively locking the agonist into the receptor. There may even be a threshold duration at the receptor after which the receptor can isomerize. Hence, it cannot be concluded that receptor residency drives efficacy or vice versa, but rather that both elements are inextricably linked.

It is clear that this correlation of long receptor residency with higher efficacy is in direct contrast to Paton's "rate theory" (Paton, 1961), where he argued that high-efficacy ligands dissociate quickly from the receptor, permitting a more rapid breakdown of the ternary complex so that the system would reset faster, allowing a second activation event to occur. There is evidence now, however, that the G protein does not necessarily dissociate from receptor, meaning that the agonist does not have to dissociate from the receptor for the G protein to dissociate (Lambert, 2008). This implies that the same agonist-receptor-G protein complex could cycle several times before dissociation of the agonist, the rate of which would depend on GDP dissociation to form the high-affinity guanine nucleotide-free complex (Scheme 1).

The present study has focused on G protein-mediated responses, but there are a growing number of examples of alternative G protein-coupled receptor signaling pathways (e.g., β-arrestin-mediated events) (Defea, 2008). It is interesting to consider whether efficacy at these other pathways might also be defined, in part, by the residency time of the agonist at the receptor. It has been shown that agonist withdrawal leads to swift dissociation of the receptor-β-arrestin2 complex, demonstrating that interaction of β-arrestin2 with the β_2 adrenoceptor is highly dependent on coincident agonist binding (Krasel et al., 2005). It is therefore plausible that an agonist that dissociates slowly from this complex may be more likely to initiate a downstream signal. There are other examples, however, in which the efficacy measured at two different pathways is not correlated (Galandrin and Bouvier, 2006), suggesting that the agonists stabilize discrete active conformations that may have different efficiencies across multiple pathways (Kenakin, 2007). Investigating the rela-

tionship between agonist off-rate and efficacy at these alternative, non-G protein-mediated pathways will be an interesting area for future investigations.

In summary, we have shown that agonist efficacy is positively correlated to duration at the receptor. This suggests that equilibrium models alone are not sufficient to describe a dynamic signaling system, and that kinetic models incorporating duration of agonist binding alongside the rate of effector activation will be required to fully explain the nature of efficacy at G protein-coupled receptors.

References

Biddlecome GH, Berstein G, and Ross EM (1996) Regulation of phospholipase C-β1 by G$_q$ and m1 muscarinic cholinergic receptor. Steady-state balance of receptor-mediated activation and GTPase-activating protein-promoted deactivation. *J Biol Chem* **271:**7999–8007.

Black JW and Leff P (1983) Operational models of pharmacological agonism. *Proc R Soc Lond B Biol Sci* **220:**141–162.

Bradford MM (1976) A rapid and sensitive method for quantitation of microgram quantities of protein utilizing principle of protein-dye binding. *Anal Biochem* **72:**248–254.

Carter CM, Leighton-Davies JR, and Charlton SJ (2007) Miniaturized receptor binding assays: complications arising from ligand depletion. *J Biomol Screen* **12:**255–266.

Cheng Y and Prusoff WH (1973) Relationship between the inhibition constant (K1) and the concentration of inhibitor which causes 50 per cent inhibition (I50) of an enzymatic reaction. *Biochem Pharmacol* **22:**3099–3108.

Cohen FR, Lazareno S, and Birdsall NJ (1996) The affinity of adenosine for the high- and low-affinity states of the human adenosine A$_1$ receptor. *Eur J Pharmacol* **309:**111–114.

Colquhoun D (1973) The relationship between classical and cooperative models for drug action, in *A Symposium on Drug Receptors* (Rang HP ed) pp 149–182, University Park Press, Baltimore.

Colquhoun D (1998) Binding, gating, affinity and efficacy: the interpretation of structure-activity relationships for agonists and of the effects of mutating receptors. *Br J Pharmacol* **125:**924–947.

Defea K (2008) Beta-arrestins and heterotrimeric G-proteins: collaborators and competitors in signal transduction. *Br J Pharmacol* **153 (Suppl 1):**S298–S309.

Del Castillo J and Katz B (1957) Interaction at end-plate receptors between different choline derivatives. *Proc R Soc London Ser B* **146:**369–381.

Dowling MR and Charlton SJ (2006) Quantifying the association and dissociation rates of unlabelled antagonists at the muscarinic M$_3$ receptor. *Br J Pharmacol* **148:**927–937.

Ehlert FJ (1985) The relationship between muscarinic receptor occupancy and adenylate cyclase inhibition in the rabbit myocardium. *Mol Pharmacol* **28:**410–421.

Galandrin S and Bouvier M (2006) Distinct signaling profiles of β1 and β2 adrenergic receptor ligands toward adenylyl cyclase and mitogen-activated protein kinase reveals the pluridimensionality of efficacy. *Mol Pharmacol* **70:**1575–1584.

Hoeren M, Brawek B, Mantovani M, Löffler M, Steffens M, van Velthoven V, and Feuerstein TJ (2008) Partial agonism at the human α_{2A}-autoreceptor: role of binding duration. *Naunyn Schmiedebergs Arch Pharmacol* **378:**17–26.

Karlin A (1967) On the application of "a plausible model" of allosteric proteins to the receptor for acetylcholine. *J Theor Biol* **16:**306–320.

Kellar KJ, Martino AM, Hall DP Jr, Schwartz RD, and Taylor RL (1985) High-affinity binding of [^{3}H]acetylcholine to muscarinic cholinergic receptors. *J Neurosci* **5:**1577–1582.

Kenakin T (2007) Functional selectivity through protean and biased agonism: who steers the ship? *Mol Pharmacol* **72:**1393–1401.

Kinzer-Ursem TL and Linderman JJ (2007) Both ligand- and cell-specific parameters control ligand agonism in a kinetic model of G protein-coupled receptor signaling. *PLoS Comput Biol* **3:**e6.

Krasel C, Bünemann M, Lorenz K, and Lohse MJ (2005) β-arrestin binding to the β2-adrenergic receptor requires both receptor phosphorylation and receptor activation. *J Biol Chem* **280:**9528–9535.

Lambert NA (2008) Dissociation of heterotrimeric G proteins in cells. *Sci Signal* **1:**re5.

Leff P (1995) The two-state model of receptor activation. *Trends Pharmacol Sci* **16:**89–97.

Lohse MJ, Nikolaev VO, Hein P, Hoffmann C, Vilardaga JP, and Bünemann M (2008) Optical techniques to analyze real-time activation and signaling of G-protein-coupled receptors. *Trends Pharmacol Sci* **29:**159–165.

Paris H, Galitzky J, and Senard JM (1989) Interactions of full and partial agonists with HT29 cell α2-adrenoceptor: comparative study of [^{3}H]UK-14,304 and [^{3}H]clonidine binding. *Mol Pharmacol* **35:**345–354.

Paton WD (1961) A theory of drug action based on rate of drug-receptor combination. *Proc R Soc Lond B Biol Sci* **154:**21–69.

Samama P, Cotecchia S, Costa T, and Lefkowitz RJ (1993) A mutation-induced activated state of the β2-adrenergic receptor. Extending the ternary complex model. *J Biol Chem* **268:**4625–4636.

Schreiber G, Henis YI, and Sokolovsky M (1985) Rate constants of agonist binding to muscarinic receptors in rat brain medulla. Evaluation by competition kinetics. *J Biol Chem* **260:**8795–8802.

Shea LD, Neubig RR, and Linderman JJ (2000) Timing is everything the role of kinetics in G protein activation. *Life Sci* **68:**647–658.

Sklar LA, Sayre J, McNeil VM, and Finney DA (1985) Competitive binding kinetics

in ligand-receptor-competitor systems. Rate parameters for unlabeled ligands for the formyl peptide receptor. *Mol Pharmacol* **28:**323–330.

Stephenson RP (1956) A modification of receptor theory. *Br J Pharmacol Chemother* **11:**379–393.

Thron CD (1973) On the analysis of pharmacological experiments in terms of an allosteric receptor model. *Mol Pharmacol* **9:**1–9.

Waelbroeck M, Boufrahi L, and Swillens S (1997) Seven helix receptors are enzymes catalysing G protein activation. What is the agonist Kact? *J Theor Biol* **187:**15–37.

Weiss JM, Morgan PH, Lutz MW, and Kenakin TP (1996) The cubic ternary complex receptor-occupancy model III. Resurrecting efficacy. *J Theor Biol* **181:**381–397.

Address correspondence to: Dr. Steven J. Charlton, Novartis Institutes for Biomedical Sciences, Wimblehurst Road, Horsham, West Sussex, UK. E-mail: steven.charlton@novartis.com